

# Boundary conditions for a divergence free velocity–pressure formulation of the Navier–Stokes equations

Jan Nordström<sup>a,b,c,\*</sup>, Ken Mattsson<sup>d</sup>, Charles Swanson<sup>e</sup>

<sup>a</sup> Department of Information Technology, Scientific Computing, Uppsala University, SE-751 05 Uppsala, Sweden

<sup>b</sup> Department of Aeronautical and Vehicle Engineering, KTH-The Royal Institute of Technology, SE-100 44 Stockholm, Sweden

<sup>c</sup> Department of Computational Physics, Division of Systems Technology, The Swedish Defense Research Agency, SE-164 90 Stockholm, Sweden

<sup>d</sup> Center for Turbulence Research, Stanford University, Stanford, CA 94305-3035, USA

<sup>e</sup> Computational Aero Sciences Branch, NASA Langley Research Center, Hampton, VA 23681, USA

Received 30 May 2006; received in revised form 9 November 2006; accepted 5 January 2007

Available online 21 January 2007

---

## Abstract

New sets of boundary conditions for the velocity–pressure formulation of the incompressible Navier–Stokes equations are derived. The boundary conditions have the same form on both inflow and outflow boundaries and lead to a divergence free solution. Moreover, the specific form of the boundary condition makes it possible to derive a symmetric positive definite equation system for the internal pressure. Numerical experiments support the theoretical conclusions.

© 2007 Elsevier Inc. All rights reserved.

*Keywords:* Navier–Stokes; Incompressible flow; Divergence; Boundary conditions

---

## 1. Introduction

Both the velocity–divergence and the velocity–pressure forms are considered when solving the incompressible Navier–Stokes equations. With the velocity–divergence form, careful consideration must be given to the discretization of the continuity equation, in order to prevent odd–even point decoupling and also to maintain the divergence free condition. Alternative methods for this form such as the vorticity/stream function formulation and the staggered grid approach are frequently applied in two dimensions. Both of these methods become less attractive in three dimensions, due to either boundary condition considerations or computational complexity.

To avoid the difficulties mentioned above and to increase the potential for computational efficiency when solving general problems, the velocity–pressure form of the equations is chosen. The main drawback with this form is that the direct enforcement of zero divergence is lost. There has been considerable discussion in

---

\* Corresponding author. Tel.: +46 8 555 0 3270; fax: +46 8 555 0 3100.

E-mail address: [Jan.Nordstrom@foi.se](mailto:Jan.Nordstrom@foi.se) (J. Nordström).

the literature regarding the proper boundary condition for the pressure equation. According to [1] the normal component of the momentum equation is the appropriate boundary condition. However, as indicated in [2,3] this particular boundary condition allows a nonzero divergence on the boundary, and thus, allows a nonzero divergence in the domain of interest. Furthermore, in [4] it is pointed out that this boundary condition provides no new information, resulting in an under-determined system. In [5] the author considers the solid boundary condition for the pressure equation and imposes the divergence or the normal derivative of the divergence in combination with the normal component of the momentum equation.

Staggered grids are often used in the numerical solution of the incompressible Navier–Stokes equations. That approach which more or less excludes the use of the energy method as an analysis tool is considered in [6–9]. Another way of dealing with the incompressible Navier–Stokes equations is to use projection or fractional step methods, see [10–12]. Typically, one first computes an approximation of the velocity field that does not satisfy the divergence relation and where no pressure is involved. Next, an approximation of the pressure is computed that is used to correct the velocity field in order to satisfy the divergence relation. These methods are very popular but in most cases low order accurate (due to the sequential computation). Yet another way to reduce the divergence is to add a term (as in [2,5]) to the pressure equation that introduce damping in the divergence equation. This technique works well, can easily complement other techniques (for example the one in this paper) and damps divergence in the whole computational domain. It might be a necessary ingredient for problems with a divergence source in the interior of the domain.

In this paper we focus more on divergence sources at the boundaries. We will revisit the problem with switching from the velocity–divergence to the velocity–pressure form and derive necessary and sufficient conditions for obtaining the same solution, see also [13]. Our approach is related to the plan of attack in [5] in the sense that we combine boundary conditions for the momentum equations with boundary conditions for the advection–diffusion equation for the divergence, and obtain a full set of boundary conditions for the velocity–pressure formulation. Our conditions are derived in the continuous setting and therefore of general use.

The rest of this paper is organized in the following way. In Section 2, we analyze the nonlinear problem and derive new boundary conditions. The results from the nonlinear problem are applied to an example in Section 3. The discrete problem is analyzed in Section 4. Numerical results are presented in Section 5. Conclusions are drawn in Section 6.

## 2. Analysis of the nonlinear problem

The initial-boundary-value problem for the two-dimensional incompressible Navier–Stokes equations on the conventional velocity–divergence form can be written as

$$\begin{aligned}
 \mathbf{V}_t + (\mathbf{V} \cdot \nabla)\mathbf{V} + \nabla p - \nu \Delta \mathbf{V} &= \mathbf{f}, & \mathbf{x} \in \Omega, & t \geq 0, \\
 \nabla \cdot \mathbf{V} &= 0, & \mathbf{x} \in \Omega, & t \geq 0, \\
 B(\mathbf{V}, p)^T &= \mathbf{g}, & \mathbf{x} \in \partial\Omega, & t \geq 0, \\
 (\mathbf{V}, p)^T &= \mathbf{h}, & \mathbf{x} \in \Omega, & t = 0,
 \end{aligned}
 \tag{1}$$

where  $\mathbf{V} = (u, v)^T$  is the fluid velocity,  $p$  is the pressure,  $\mathbf{f}$  is the forcing function,  $\mathbf{g}$  the boundary data and  $\mathbf{h} = (h_1, h_2)^T$  the initial data.  $\nabla$  and  $\Delta$  are the gradient and Laplacian operators respectively. The density is taken to be one, and the coefficient  $\nu$  is the reciprocal of the Reynolds number,  $\nu = 1/Re$ . The domain  $\Omega$  is in  $\mathfrak{R}^2$ , and the boundary of the domain is  $\partial\Omega$ . The two boundary conditions are represented by the boundary operator  $B(\mathbf{V}, p)$  and the boundary data  $\mathbf{g}$ .

There are alternative forms for the system (1). One of these forms can be derived by taking the divergence of the momentum equation and applying  $\nabla \cdot \mathbf{V} = 0$ . The resulting system is called the velocity–pressure (or pressure Poisson) form of the equations, and the associated initial-boundary-value problem is defined by

$$\begin{aligned}
 \mathbf{V}_t + (\mathbf{V} \cdot \nabla)\mathbf{V} + \nabla p - \nu \Delta \mathbf{V} &= \mathbf{f}, & \mathbf{x} \in \Omega, & t \geq 0, \\
 \Delta p &= \tilde{\mathbf{f}}, & \mathbf{x} \in \Omega, & t \geq 0,
 \end{aligned}$$

$$\begin{aligned}
B(\mathbf{V}, p)^T &= \mathbf{g}, & \mathbf{x} \in \partial\Omega, & t \geq 0, \\
\tilde{B}(\mathbf{V}, p)^T &= \tilde{\mathbf{g}}, & \mathbf{x} \in \partial\Omega, & t \geq 0, \\
(\mathbf{V}, p)^T &= \mathbf{h}, & \mathbf{x} \in \Omega, & t = 0,
\end{aligned} \tag{2}$$

where  $\tilde{\mathbf{f}} = (\nabla \cdot \mathbf{f} - (\nabla u \cdot \mathbf{V}_x + \nabla v \cdot \mathbf{V}_y))$ . Now, the pressure equation plays the role of the continuity equation. Since this equation is in second-order form, the system requires an additional boundary condition (with boundary operator  $\tilde{B}$ ).

Note that even though one can derive the pressure Poisson equation by assuming zero divergence, it is not clear that the implication goes the other way. In other words, the simple replacement of divergence relation with the pressure equation *does not* imply zero divergence. Other elements must also be considered. The main part of this paper is devoted to a step by step derivation (using classical initial boundary value theory) of why (2) is an appropriate form of (1) and what kind of boundary conditions ( $\tilde{B}$  and  $\tilde{\mathbf{g}}$ ) and initial conditions ( $\mathbf{h}$ ) the system (2) requires in order to produce identically the same solution as the one given by (1).

### 2.1. Replacing the divergence condition

Let us start by considering the well posedness of a time-dependent scalar advection–diffusion equation with a general set of data

$$\begin{aligned}
\phi_t + (\vec{U} \cdot \nabla)\phi - v\Delta\phi &= \mathbf{F}, & \mathbf{x} \in \Omega, & t \geq 0, \\
L\phi &= \mathbf{G}, & \mathbf{x} \in \partial\Omega, & t \geq 0, \\
\phi &= \mathbf{H}, & \mathbf{x} \in \Omega, & t = 0.
\end{aligned} \tag{3}$$

The data in (3) are the forcing function  $\mathbf{F}$ , the boundary data  $\mathbf{G}$  and the initial data  $\mathbf{H}$ . For reasons that become evident later we require  $\mathbf{H}$  to be small. Also unknown in (3) is the boundary operator  $L$ . For the variable coefficient case,  $\vec{U} = (a, b)$  varies in space and time while for the nonlinear case we have  $\vec{U} = (u, v)$  and  $\phi = \nabla \cdot \vec{U}$ . The viscosity  $v \ll 1$  is constant and small.

**Remark.** Consider the problem (1). By taking the divergence of the momentum equation and *not* imposing the divergence condition we obtain the advection–diffusion problem (3) where  $\phi = \nabla \cdot \mathbf{V}$ ,  $\vec{U} = \mathbf{V}$  and  $\mathbf{F} = \tilde{\mathbf{f}} - \Delta p$ . However, and we stress this point, we will first consider (3) as a fully general advection–diffusion problem and determine general conditions that leads to  $\phi = 0$ . Once that is done, we can relate that general result to the specific Navier–Stokes formulation (2) and explicitly state the conditions that are required for obtaining zero divergence. This is the main theme of the paper.

The energy method (multiply with  $\phi$ , integrate over the domain and apply Green’s theorem) applied to (3) yields

$$\|\phi\|_t^2 + 2v \int_{\Omega} |\nabla\phi|^2 \, dx \, dy = - \oint_{\partial\Omega} [(\vec{U} \cdot \vec{n})\phi^2 - 2v\phi \frac{\partial\phi}{\partial n}] \, ds + \int_{\Omega} [(\nabla \cdot \vec{U})\phi^2 + 2\phi\mathbf{F}] \, dx \, dy, \tag{4}$$

where  $\vec{n}$  is the outward pointing normal. Clearly we need to bound the two terms on the right-hand side of (4).

Let us start with the boundary integral and assume that  $U_n = \vec{U} \cdot \vec{n} \neq 0$ . We rewrite the boundary terms as

$$U_n\phi^2 - 2v\phi \frac{\partial\phi}{\partial n} = U_n^{-1} \left[ \left( U_n\phi - v \frac{\partial\phi}{\partial n} \right)^2 - \left( v \frac{\partial\phi}{\partial n} \right)^2 \right]. \tag{5}$$

A boundary condition that cancels the quadratic form with the wrong sign in (4) is

$$\tilde{B}(\mathbf{V}, p)^T = L\phi = \frac{(U_n - |U_n|)}{2} \phi - v \frac{\partial\phi}{\partial n} = \mathbf{G}. \tag{6}$$

The boundary condition (6) yields the estimate

$$- \oint_{\partial\Omega} \left[ U_n\phi^2 - 2v\phi \frac{\partial\phi}{\partial n} \right] \, ds \leq \oint_{\partial\Omega} \frac{1}{|U_n|} (\mathbf{G}^2 - (|U_n|\phi + \mathbf{G})^2) \, ds \tag{7}$$

both for inflow ( $U_n < 0$ ) and outflow ( $U_n > 0$ ).

**Remark.** Other possible boundary conditions (that include the case where  $U_n = 0$ ) except (6) that can be used are  $\phi = 0$  both for inflow and outflow and  $\partial\phi/\partial n = 0$  for outflow. However, (6) is the most dissipative condition.

Next we consider the second potential growth term in (4). We get the estimate

$$\int_{\Omega} [(\nabla \cdot \vec{U})\phi^2 + 2\phi\mathbf{F}] \, dx \, dy \leq (\eta + \delta)\|\phi\|^2 + \frac{1}{\eta}\|\mathbf{F}\|^2 \tag{8}$$

by using  $2\phi\mathbf{F} = -(\sqrt{\eta}\phi - \mathbf{F}/\sqrt{\eta})^2 + \eta\phi^2 + \mathbf{F}^2/\eta$ . For the linear problem we have  $\delta = |\nabla \cdot \vec{U}|_{\max}$ . To get an estimate in the nonlinear problem we consider short times  $t \leq T_0$  and recall that  $\phi(x, 0) = \mathbf{H}$  where  $\mathbf{H}$  is small. Note also that  $\phi$  obeys a maximum principle (the magnitude of local maxima and minima decrease). This implies that  $\phi$  is limited for short times and consequently we can choose  $\delta = |\phi|_{\max}$  for  $t \leq T_0$  and  $\mathbf{x} \in \partial\Omega$ .

By defining the boundary norm as  $\|\mathbf{U}\|_{\partial\Omega}^2 = \oint_{\partial\Omega} \mathbf{U}^2/|U_n| \, ds$ , introducing the notation  $\tilde{\eta} = \eta + \delta$  and inserting (7), (8) into (4) we obtain the final estimate

$$\|\phi\|^2 + \int_0^T (2\nu\|\nabla\phi\|^2 + \| |U_n|\phi + \mathbf{G}\|_{\partial\Omega}^2) e^{-\tilde{\eta}(t-T)} \, dt \leq \|\mathbf{H}\|^2 e^{\tilde{\eta}T} + \int_0^T \left( \frac{1}{\tilde{\eta}}\|\mathbf{F}\|^2 + \|\mathbf{G}\|_{\partial\Omega}^2 \right) e^{-\tilde{\eta}(t-T)} \, dt. \tag{9}$$

The estimate (9) is obtained by multiplying both sides of (4) with the integrating factor  $e^{-\tilde{\eta}t}$ , forming a total time derivative and finally integrating from 0 to  $T$ . In the nonlinear case, (9) is valid for  $T \leq T_0$ .

We are now ready to prove the following proposition.

**Proposition 2.1.**

*Consider the problem (3). If the boundary conditions are given by (6) and*

$$\mathbf{F} = 0, \quad \mathbf{G} = 0, \quad \mathbf{H} = 0 \tag{10}$$

*then the  $L_2$  norm of the divergence  $\|\phi\|^2$  will be zero for all times.*

**Proof.** The conditions (10) inserted into (9) yields

$$\|\phi\|^2 + \int_0^T (2\nu\|\nabla\phi\|^2 + \| |U_n|\phi\|_{\partial\Omega}^2) e^{-\tilde{\eta}(t-T)} \, dt \leq 0. \tag{11}$$

In the linear case this concludes the proof. In the nonlinear case, (11) is valid for small times  $T \leq T_0$  and we obtain  $\|\phi\|^2(T_0) = 0$ . A repetition of the argument proves Proposition 2.1 for the nonlinear case for all times.  $\square$

**Remark.** Note that for long time calculations,  $\mathbf{H} \neq 0$  but sufficiently small might suffice since initial nonzero divergence effects will decay with time due to the dissipative effect of the boundary condition (6), see (7), (8) and (4).

*2.2. The energy estimate for the momentum equations*

Multiplication of the top two equations in (2) with  $\mathbf{V}$  and integration over the domain yields

$$\|\mathbf{V}\|_t^2 + 2\nu(\|\nabla u\|^2 + \|\nabla v\|^2) = - \oint_{\partial\Omega} W^T A(\mathbf{V}) W \, ds + 2 \int_{\Omega} [\phi(p + \mathbf{V}^2/2) + \mathbf{V} \cdot \mathbf{f}] \, dx \, dy, \tag{12}$$

where  $\phi = \nabla \cdot \mathbf{V}$  and

$$W = \begin{pmatrix} u_n \\ u_s \\ p \\ v(\partial u_n/\partial n) \\ v(\partial u_s/\partial n) \end{pmatrix}, \quad A(\mathbf{V}) = \begin{pmatrix} u_n & 0 & +1 & -1 & 0 \\ 0 & u_n & 0 & 0 & -1 \\ +1 & 0 & 0 & 0 & 0 \\ -1 & 0 & 0 & 0 & 0 \\ 0 & -1 & 0 & 0 & 0 \end{pmatrix}. \tag{13}$$

In (12) and (13)  $u_n, u_s$  denote the normal velocity and tangential velocity. By choosing the boundary conditions and initial data discussed in the previous section we have  $\phi = 0$ .

To bound the energy in (12) we need to make sure that  $W^T A W \leq 0$ . The correct number of boundary conditions and a maximally dissipative form of the boundary conditions are obtained by specifying the correct characteristic variable, for more details see [14]. We can write the condition in diagonal form as

$$W^T A W = (X^T W)^T \Lambda (X^T W)^T$$

and specify  $(X^T W)_i = C_i$  whenever  $\lambda_i < 0$ . Straightforward but tedious algebra yields

$$\lambda_{1,2} = \frac{u_n}{2} \pm \sqrt{\left(\frac{u_n}{2}\right)^2 + 1}, \quad \lambda_3 = 0, \quad \lambda_{4,5} = \frac{u_n}{2} \pm \sqrt{\left(\frac{u_n}{2}\right)^2 + 2}, \tag{14}$$

$$X^T = \begin{bmatrix} \sqrt{1 + \lambda_1^2} & 0 & 0 & 0 & 0 \\ 0 & \sqrt{1 + \lambda_2^2} & 0 & 0 & 0 \\ 0 & 0 & \sqrt{2} & 0 & 0 \\ 0 & 0 & 0 & \sqrt{2 + \lambda_4^2} & 0 \\ 0 & 0 & 0 & 0 & \sqrt{2 + \lambda_5^2} \end{bmatrix}^{-1} \begin{bmatrix} 0 & \lambda_1 & 0 & 0 & -1 \\ 0 & \lambda_2 & 0 & 0 & -1 \\ 0 & 0 & 1 & 1 & 0 \\ \lambda_4 & 0 & 1 & -1 & 0 \\ \lambda_5 & 0 & 1 & -1 & 0 \end{bmatrix}. \tag{15}$$

Note that  $\lambda_2, \lambda_5$  are negative for all values of  $u_n$ . This implies that the conditions

$$C_2 = \lambda_2 u_s - v \frac{\partial u_s}{\partial n} = g_2, \quad C_5 = \lambda_5 u_n - v \frac{\partial u_n}{\partial n} + p = g_5, \tag{16}$$

lead to well posedness. Our result can be formulated as

$$B(\mathbf{V}, p)^T = \begin{pmatrix} 0 & \lambda_2 - v\partial/\partial n & 0 \\ \lambda_5 - v\partial/\partial n & 0 & 1 \end{pmatrix} \begin{pmatrix} u_n \\ u_s \\ p \end{pmatrix} = \mathbf{g}. \tag{17}$$

**Remark.** Note that (16) and (17) can be imposed on both inflow and outflow boundaries which simplifies numerical calculations since it is not necessary to switch type of boundary conditions. For other types of boundary conditions that lead to well-posedness, see [15,16].

**Remark.** To apply the boundary conditions (16) and (17), the right-hand side  $\mathbf{g}$  which includes both the pressure and the normal gradients of the velocities must be known (or at least a fair guess must be available). In many practical problems, pressure data is given and one can assume that the contribution from the velocity gradients is small. One example is the inflow/outflow problem of a jet-engine. Typical data (provided e.g. by the engine companies) at the inflow are the total pressure, the total temperature and the flow direction (or mass flow rate [17,18]) and at the outlet the static pressure. At solid boundaries, our boundary conditions are not applicable since neither the pressure nor the normal gradients of the velocities are known (or can be estimated). However, one can easily combine (16) with the wall boundary technique presented in [2,5] in order to treat all boundaries appropriately.

By choosing the boundary conditions (17) we obtain the final estimate

$$\begin{aligned} \|\mathbf{V}\|^2 + \int_0^T 2v(\|\nabla u\|^2 + \|\nabla v\|^2)e^{-\eta(t-T)} + \int_0^T \|C^+\|_r^2 e^{-\eta(t-T)} dt \\ \leq \|\mathbf{h}\|^2 e^{\eta T} + \int_0^T \left(\frac{1}{\eta}\|\mathbf{f}\|^2 + \|\mathbf{g}\|_r^2\right)e^{-\eta(t-T)} dt, \end{aligned} \tag{18}$$

where  $\|C^+\|_r^2 = \sum_{i=1,3,4} \int_\Gamma \lambda_i C_i^2 ds$ ,  $\|\mathbf{g}\|_r^2 = \sum_{i=2,5} \int_\Gamma |\lambda_i| g_i^2 ds$  and  $\Gamma = \partial\Omega$ .

2.3. *The velocity–pressure formulation for zero divergence*

The main result in this paper is

**Proposition 2.2.** *Consider the velocity–pressure formulation (2). If the boundary conditions are given by (6) and (17) with  $\tilde{\mathbf{g}} = 0$  and  $\nabla \cdot \mathbf{h}_1 = 0$ . Then (2) has a divergence free solution that satisfies the estimate (18).*

**Proof.** See Sections 2.2 and 2.3 above.  $\square$

**Remark.** The linearized version of (2) can (by using the estimate (18)) be shown to have a unique solution and hence be strongly well-posed, see also [15,19] where similar results were obtained. We can summarize the result in Propositions 2.1 and 2.2 in the following way. By

- solving Poisson’s equation for the pressure ( $\mathbf{F} = \tilde{\mathbf{f}} - \Delta p = 0$ ),
- using dissipative ( $B$ ) boundary conditions for the momentum equations,
- using dissipative ( $\tilde{B}$ ) boundary conditions for the divergence equation,
- using zero boundary data ( $\tilde{\mathbf{g}} = 0$ ) for the divergence boundary conditions,
- initializing with a divergence free velocity field ( $\nabla \cdot \mathbf{h}_1 = 0$ ), a divergence-free solution to the velocity–pressure formulation (2) will be obtained.

3. **An example**

In this section we will investigate the new boundary conditions in some detail by using the Laplace–Fourier transform technique on a constant coefficient version of problem (1) and (2). By Laplace–Fourier transforming these problems, we get two systems of ordinary differential equations of the form

$$\mathbf{A}V_{xx} + \mathbf{B}V_x + \mathbf{C}V = \tilde{\mathbf{F}}, \quad x \geq 0. \tag{19}$$

In (19),  $\tilde{\mathbf{F}}$  includes the Laplace–Fourier transformed forcing functions and initial data present in (1) and (2).  $V$  is the Laplace–Fourier transform of  $(\mathbf{V}, p)^T$ . The constant matrices in (19) are

$$\mathbf{A} = \begin{pmatrix} -v & 0 & 0 \\ 0 & -v & 0 \\ 0 & 0 & -1 \end{pmatrix}, \quad \mathbf{B} = \begin{pmatrix} \bar{u} & 0 & 1 \\ 0 & \bar{u} & 0 \\ 0 & 0 & 0 \end{pmatrix}, \quad \mathbf{C} = \begin{pmatrix} \tilde{s} & 0 & 0 \\ 0 & \tilde{s} & i\omega \\ 0 & 0 & \omega^2 \end{pmatrix}, \tag{20}$$

$$\mathbf{A} = \begin{pmatrix} -v & 0 & 0 \\ 0 & -v & 0 \\ 0 & 0 & 0 \end{pmatrix}, \quad \mathbf{B} = \begin{pmatrix} \bar{u} & 0 & 1 \\ 0 & \bar{u} & 0 \\ 1 & 0 & 0 \end{pmatrix}, \quad \mathbf{C} = \begin{pmatrix} \tilde{s} & 0 & 0 \\ 0 & \tilde{s} & i\omega \\ 0 & i\omega & 0 \end{pmatrix}, \tag{21}$$

for the velocity–pressure and velocity–divergence form respectively. The constants and parameters  $\bar{u}$ ,  $\bar{v}$ ,  $v$ ,  $s$ ,  $i\omega$  in (20) and (21) are the velocity components in  $x$ ,  $y$ -direction, the viscosity, the dual variable to time and the dual variable to  $y$  respectively. We have also used the abbreviation  $\tilde{s} = s + i\omega\bar{v} + v\omega^2$ .

We limit the analysis to the case where  $|\omega| \geq \omega_0 > 0$  since the equations collapse for  $\omega = 0$ . This means that we exclude solutions with zero mean value in the  $y$ -direction. The top two rows are identical for both formulations and represent the momentum equations. The bottom row represents the Poisson equation for the pressure and the divergence relation respectively.

The system (19) defined in the half space  $x \geq 0$  must be augmented with boundary conditions. At infinity ( $x \rightarrow \infty$ ) we demand a bounded solution which implies that only decaying modes will be considered. At  $x = 0$  we impose boundary conditions.

The solution is a sum of the homogeneous and particular solution, i.e.  $V = U + U_p$ . The particular solution  $U_p$  is a smooth bounded function of the data of the problem, i.e.  $U_p = U_p(\tilde{\mathbf{F}})$ . We assume that the data have

compact support in  $x \geq 0$ , i.e. that  $\tilde{\mathbf{F}}(|\mathbf{x}| > R) = 0$ . The homogeneous solution is obtained by making the ansatz  $U = \phi \exp(\kappa x)$  and inserting that into the homogeneous version of (19). That gives us the generalized eigenvalues and eigenvectors as solutions to

$$|\mathbf{A}\kappa_i^2 + \mathbf{B}\kappa_i + \mathbf{C}| = 0, \quad (\mathbf{A}\kappa_i^2 + \mathbf{B}\kappa_i + \mathbf{C})\phi_i = 0, \tag{22}$$

where  $i = 1-6$  for the velocity–pressure case and  $i = 1-4$  for the velocity–divergence case.

### 3.1. The velocity–pressure formulation

In the velocity–pressure case we get

$$\kappa_{1,2} = \pm|\omega|, \quad \kappa_{3,4,5,6} = \left(\frac{\bar{u}}{2v}\right) \pm \sqrt{\left(\frac{\bar{u}}{2v}\right)^2 + \frac{\tilde{s}}{v}}. \tag{23}$$

The double roots  $\kappa_{3,4,5,6}$  indicate that  $U = (\phi_0 + x\phi_1)\exp(\kappa_{3,4,5,6}x)$  is the proper ansatz. By using that ansatz we get  $\phi_0 = 0$  and the solution

$$U = \sum_{i=1}^6 \sigma_i \psi_i e^{\kappa_i x}, \tag{24}$$

where the  $\sigma_i$ 's are constant to be determined by the boundary conditions and

$$\psi_1 = \begin{bmatrix} 1 \\ +\frac{\omega}{|\omega|} \\ -\frac{\beta_1}{|\omega|} \end{bmatrix}, \quad \psi_2 = \begin{bmatrix} 1 \\ -\frac{\omega}{|\omega|} \\ +\frac{\beta_2}{|\omega|} \end{bmatrix}, \quad \psi_3 = \psi_5 = \begin{bmatrix} 1 \\ 0 \\ 0 \end{bmatrix}, \quad \psi_4 = \psi_6 = \begin{bmatrix} 0 \\ 1 \\ 0 \end{bmatrix}. \tag{25}$$

The parameters in (25) are defined as  $\beta_1 = \tilde{s} + \bar{u}|\omega| - v|\omega|^2$ ,  $\beta_2 = \tilde{s} - \bar{u}|\omega| - v|\omega|^2$ . A decaying solution for a positive real part in  $s$  and positive  $x$  is

$$U = \sigma_2 \psi_2 e^{\kappa_2 x} + (\sigma_5 \psi_5 + \sigma_6 \psi_6) e^{\kappa_5 x}. \tag{26}$$

There is a possibility of a triple root case (for a more detailed discussion on multiple roots, see [16]) since the parameters  $\beta_1, \beta_2$  might vanish. For that case we have

$$\begin{aligned} \kappa_{34} &= \kappa_1 + \sqrt{\left(\frac{\bar{u}}{2v} - |\omega|\right)^2 + \frac{\beta_1}{v}} - \left(\frac{\bar{u}}{2v} - |\omega|\right), \\ \kappa_{56} &= \kappa_2 - \sqrt{\left(\frac{\bar{u}}{2v} + |\omega|\right)^2 + \frac{\beta_2}{v}} + \left(\frac{\bar{u}}{2v} + |\omega|\right). \end{aligned} \tag{27}$$

The triple root ansatz  $U = (\phi_0 + x\phi_1 + x^2\phi_2)\exp(\kappa_2 x)$  yields the decaying solution

$$U = \begin{bmatrix} c_1 \\ c_2 \\ c_3 \end{bmatrix} + x c_3 \begin{bmatrix} \frac{|\omega|}{\bar{u}+2v|\omega|} \\ -\frac{i\omega}{\bar{u}+2v|\omega|} \\ 0 \end{bmatrix} e^{-|\omega|x}. \tag{28}$$

By writing the decaying double root solution (26) in a modified way as

$$U = \frac{\sigma_2}{\kappa_5 - \kappa_2} \psi_2 e^{\kappa_2 x} + \left[ \begin{bmatrix} \sigma_5 \\ \sigma_6 \\ 0 \end{bmatrix} - \frac{\sigma_2}{\kappa_5 - \kappa_2} \begin{bmatrix} 1 \\ -\frac{i\omega}{|\omega|} \\ 0 \end{bmatrix} \right] e^{\kappa_5 x}, \tag{29}$$

using (27), making the substitutions  $c_1 = \sigma_5$ ,  $c_2 = \sigma_6$  and  $c_3 = -\sigma_2 \frac{\bar{u}+2v|\omega|}{|\omega|}$  and letting  $\beta_2 \rightarrow 0$  we find that (29) converge to (28).

### 3.2. The velocity–divergence formulation

Essentially the same procedure as described above yields the four generalized eigenvalues

$$\kappa_{1,2} = \pm|\omega|, \quad \kappa_{3,5} = \left(\frac{\bar{u}}{2\nu}\right) \pm \sqrt{\left(\frac{\bar{u}}{2\nu}\right)^2 + \frac{\tilde{s}}{\nu}}. \tag{30}$$

The numbering in (30) is chosen to simplify the comparison with the velocity–pressure formulation above. Without going into detail, we state that the decaying single root solution that converges to the double root solution is

$$U = \frac{\alpha_2}{\kappa_5 - \kappa_2} \psi_2 e^{\kappa_2 x} + \left(\alpha_5 - \frac{\alpha_2}{\kappa_5 - \kappa_2}\right) \begin{bmatrix} 1 \\ \frac{i\kappa_5}{\omega} \\ 0 \end{bmatrix} e^{\kappa_5 x}. \tag{31}$$

Again we use the notation established in the previous section.

### 3.3. The effect of the new boundary conditions

Now we will investigate what effect the divergence boundary condition (6) has on the velocity–pressure solution. We can prove

**Proposition 3.1.**

*Consider the velocity–pressure formulation (29). By applying the divergence boundary condition (6) we obtain the divergence free solution given in (31).*

**Proof.** The boundary condition (6) applied on the boundary  $x = 0$  with the outward normal pointing in the negative  $x$ -direction and the velocity  $\mathbf{V} = (\bar{u}, \bar{v})^T$  is

$$\left(\frac{\bar{u} + |\bar{u}|}{2}\right) \phi - \nu \phi_x = 0. \tag{32}$$

With  $\bar{u} > 0$  we have inflow and a Robin boundary condition while  $\bar{u} < 0$  yields a clean Neumann condition. Both cases can be treated simultaneously, and (32) applied to (29) yields

$$\sigma_6 = \frac{1}{i\omega} \sigma_2 - \frac{\kappa_5}{i\omega} \sigma_5,$$

which inserted in (29) yields (31) exactly.  $\square$

An almost immediate consequence of Proposition 3.1 is

**Lemma 3.2.** *The divergence free form of the velocity–pressure formulation augmented with the boundary conditions (17) yields a pointwise bounded solution.*

**Proof.** The boundary conditions (17) leads to an energy estimate of the form (18) which bounds the velocity components in Laplace–Fourier space pointwise. By normalizing the eigenvectors in (31) with  $|\psi_2|$  we get

$$U = \frac{\tilde{\alpha}_2}{\kappa_5 - \kappa_2} \frac{1}{|\psi_2|} \psi_2 e^{\kappa_2 x} + \left(\tilde{\alpha}_5 - \frac{\tilde{\alpha}_2}{\kappa_5 - \kappa_2}\right) \frac{1}{|\psi_2|} \begin{bmatrix} 1 \\ \frac{i\kappa_5}{\omega} \\ 0 \end{bmatrix} e^{\kappa_5 x}. \tag{33}$$

The boundedness of the velocity components now implies that the coefficients  $\tilde{\alpha}_2, \tilde{\alpha}_5$  are bounded. This in turn implies that the pressure is also bounded since

$$p = \tilde{\alpha}_2 \frac{\beta_2}{(\kappa_5 - \kappa_2)|\omega|} \frac{1}{|\psi_2|} e^{\kappa_2 x}$$

and  $|\omega| > \omega_0 > 0$ . The inverse Laplace–Fourier transform yields the same result in the nontransformed space.  $\square$

### 4. The numerical approximation

The result of the analysis will be evaluated by using a high order finite difference technique. To construct the scheme we use one-dimensional summation-by-parts (SBP) operators. To make the paper self-contained we start with a short description (for more details see [20–22]). We define the first and second derivative operators of interest in this paper.

**Definition 4.1.**

A difference operator  $D_1 = H^{-1}Q$  approximating  $\partial/\partial x$  is a first derivative SBP operator if  $H = H^T > 0$  and  $Q + Q^T = B = \text{diag}(-1, 0, \dots, 0, 1)$ .

**Definition 4.2.** A difference operator  $D_2 = H^{-1}(-M + BS)$  approximating  $\partial^2/\partial x^2$  is said to be a symmetric second derivative SBP operator if  $M = M^T \geq 0$ , if  $S$  includes an approximation of the first derivative operator at the boundary and  $B = \text{diag}(-1, 0, \dots, 0, 1)$ .

The first and second derivative operators in this paper are based on diagonal norms. They are half as accurate at the boundaries as in the interior. The theory in [23] implies that first derivative operators of order 4, 6, 8 lead to globally 3, 4, 5th order accurate schemes for hyperbolic problems and 4, 5, 6th order global accuracy for parabolic problems.

We consider a two-dimensional domain with an  $N + 1 \times M + 1$ -points equidistant grid. The numerical approximation at grid point  $(x_i, y_j)$  is denoted  $v_{i,j}$ . We define a discrete solution vector  $v^T = [v^0, v^1, \dots, v^N]$ , where  $v^k = [v_{k,0}, v_{k,1}, \dots, v_{k,M}]$  is the solution vector at  $x_k$  along the  $y$ -direction, as illustrated in Fig. 1. To simplify the notation we introduce  $v_{w,e,s,n}$ , to define the boundary values at the west, east, south and north boundaries (see Fig. 1). To distinguish if a difference operator  $D$  is operating in the  $x$  or  $y$ -directions we use the notations  $D_x$  and  $D_y$ . The following two-dimensional operators:

$$\begin{aligned} D_x &= (D_1 \otimes I_y), & D_y &= (I_x \otimes D_1), \\ D_{2x} &= (D_2 \otimes I_y), & D_{2y} &= (I_x \otimes D_2), \\ H_x &= (H \otimes I_y), & H_y &= (I_x \otimes H), \end{aligned} \tag{34}$$

will be frequently used.  $D_1, D_2$  and  $H$  are the one-dimensional operators discussed above and  $I_{x,y}$  are the identity matrices. All matrices have the appropriate size in the  $x$  and  $y$ -direction respectively. We have introduced the Kronecker product

$$C \otimes D = \begin{bmatrix} c_{0,0}D & \cdots & c_{0,q-1}D \\ \vdots & & \vdots \\ c_{p-1,0}D & \cdots & c_{p-1,q-1}D \end{bmatrix},$$

where  $C$  is a  $p \times q$  matrix and  $D$  is a  $m \times n$  matrix. Two useful rules for the Kronecker product are  $(A \otimes B)(C \otimes D) = (AC) \otimes (BD)$  and  $(A \otimes B)^T = A^T \otimes B^T$ .

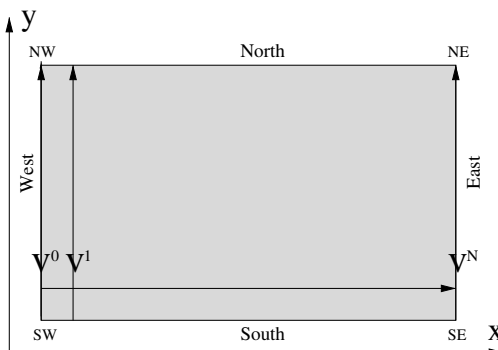


Fig. 1. Two-dimensional domain showing the orientation of the solution vectors.

**4.1. The semi-discrete approximation**

The semi-discrete finite difference approximation (including a skew-symmetric splitting of the convective terms) of the momentum equations can be written

$$\begin{aligned}
 u_t + D_x^{(\text{skew})}u + D_y^{(\text{skew})}u + D_x p &= \nu D_L u + \text{SAT}^{(u)} + F^{(u)}, \\
 v_t + D_x^{(\text{skew})}v + D_y^{(\text{skew})}v + D_y p &= \nu D_L v + \text{SAT}^{(v)} + F^{(v)}.
 \end{aligned}
 \tag{35}$$

In (35),  $F^{(u,v)}$  are the discrete forcing functions, and  $D_{x,y}^{\text{skew}}$  the skew-symmetric split operator in the  $x$ - and  $y$ -direction, respectively

$$D_x^{(\text{skew})} \equiv \frac{1}{2}AD_x + \frac{1}{2}D_xA - \frac{1}{2}A_x, \quad D_y^{(\text{skew})} \equiv \frac{1}{2}BD_y + \frac{1}{2}D_yB - \frac{1}{2}B_y.$$

The matrices  $A, B, A_x, B_y$  have the values of  $u, v, D_x u, D_y v$  injected on the diagonal. We have also introduced  $D_L = D_{2x} + D_{2y}$ , which is the discrete Laplacian. The boundary conditions are introduced as penalty terms  $\text{SAT}^{(u,v)}$ , using the SAT method, see for example [24,25,22]. The discrete Poisson system for the pressure, see Eq. (2), is given by

$$D_L p = f, \tag{36}$$

where  $f = -(D_x u)(D_x u) + 2(D_y u)(D_x v) + (D_y v)(D_y v) + D_x F^{(u)} + D_y F^{(v)}$ .

**4.2. Boundary conditions for the semi-discrete approximation**

The discrete version of the boundary condition (6) that leads to maximum dissipation of the divergence  $u_x + v_y = \phi$  is given by

$$\begin{aligned}
 L_w^{(\phi)} &= \frac{(u + |u|)}{2} (D_x u + D_y v)_w - \nu (D_x (D_x u + D_y v))_w = 0, \\
 L_e^{(\phi)} &= \frac{(u - |u|)}{2} (D_x u + D_y v)_e - \nu (D_x (D_x u + D_y v))_e = 0, \\
 L_s^{(\phi)} &= \frac{(v + |v|)}{2} (D_x u + D_y v)_s - \nu (D_y (D_x u + D_y v))_s = 0, \\
 L_n^{(\phi)} &= \frac{(v - |v|)}{2} (D_x u + D_y v)_n - \nu (D_y (D_x u + D_y v))_n = 0.
 \end{aligned}
 \tag{37}$$

**Remark.** Other possible boundary conditions except (37) that can be used are  $(D_x u + D_y v) = 0$  both for inflow and outflow and  $\partial(D_x u + D_y v)/\partial n = 0$  for outflow.

The discrete boundary conditions for the  $x$ -component  $u$ , at the boundaries are given by

$$\begin{aligned}
 L_w^{(u)} &= -\lambda_5^{(w)} u_w - \nu (Su)_w + p_w = g_w^{(u)}, \\
 L_e^{(u)} &= +\lambda_5^{(e)} u_e - \nu (Su)_e + p_e = g_e^{(u)}, \\
 L_s^{(u)} &= -\lambda_2^{(s)} u_s - \nu (Su)_s = g_s^{(u)}, \\
 L_n^{(u)} &= +\lambda_2^{(n)} u_n - \nu (Su)_n = g_n^{(u)}.
 \end{aligned}
 \tag{38}$$

The corresponding boundary conditions for the  $y$ -component  $v$  are given by

$$\begin{aligned}
 L_w^{(v)} &= -\lambda_2^{(w)} v_w - \nu (Sv)_w = g_w^{(v)}, \\
 L_e^{(v)} &= +\lambda_2^{(e)} v_e - \nu (Sv)_e = g_e^{(v)}, \\
 L_s^{(v)} &= -\lambda_5^{(s)} v_s - \nu (Sv)_s + p_s = g_s^{(v)}, \\
 L_n^{(v)} &= +\lambda_5^{(e)} v_n - \nu (Sv)_n + p_n = g_n^{(v)}.
 \end{aligned}
 \tag{39}$$

The expressions for the two eigenvalues  $\lambda_{2,5}$  are given by (15), and at each boundary, we get,

$$\begin{aligned} \lambda_5^{(w)} &= \frac{-u_w}{2} - \sqrt{\left(\frac{-u_w}{2}\right)^2 + 2}, & \lambda_2^{(w)} &= \frac{-u_w}{2} - \sqrt{\left(\frac{u_w}{2}\right)^2 + 1}, \\ \lambda_5^{(e)} &= \frac{u_e}{2} - \sqrt{\left(\frac{u_e}{2}\right)^2 + 2}, & \lambda_2^{(e)} &= \frac{u_e}{2} - \sqrt{\left(\frac{u_e}{2}\right)^2 + 1}, \\ \lambda_5^{(s)} &= \frac{-v_s}{2} - \sqrt{\left(\frac{-v_s}{2}\right)^2 + 2}, & \lambda_2^{(s)} &= \frac{-v_s}{2} - \sqrt{\left(\frac{-v_s}{2}\right)^2 + 1}, \\ \lambda_5^{(n)} &= \frac{v_n}{2} - \sqrt{\left(\frac{v_n}{2}\right)^2 + 2}, & \lambda_2^{(n)} &= \frac{v_n}{2} - \sqrt{\left(\frac{v_n}{2}\right)^2 + 1}. \end{aligned} \tag{40}$$

The penalty terms for the  $x$ - and  $y$ -component  $(u, v)$  are given by

$$\begin{aligned} \text{SAT}^{(u,v)} &= \tau_w^{(u,v)} H_x^{-1} e_0 \otimes (L_w^{(u,v)} - g_w^{(u,v)}) + \tau_e^{(u,v)} H_x^{-1} e_N \otimes (L_e^{(u,v)} - g_e^{(u,v)}) + \tau_s^{(u,v)} H_y^{-1} (L_s^{(u,v)} - g_s^{(u,v)}) \otimes e_0 \\ &\quad + \tau_n^{(u,v)} H_y^{-1} (L_n^{(u,v)} - g_n^{(u,v)}) \otimes e_N, \end{aligned}$$

where  $e_0 = [1, 0, \dots, 0]^T$ ,  $e_N = [0, \dots, 0, 1]^T$ . The eight penalty parameters,  $\tau_{w,e,s,n}^{(u,v)}$  will be tuned to obtain an energy estimate. By multiplying the first and the second equation in (35) by  $u^T \bar{H}$  and  $v^T \bar{H}$  respectively and adding the transpose we obtain,

$$(\|u\|_{\bar{H}}^2 + \|v\|_{\bar{H}}^2)_t = BT + DI + RT. \tag{41}$$

In (41),  $\bar{H} \equiv H_x H_y$  denotes the two-dimensional norm. The  $BT$  quantities denote the boundary terms that will be discussed below. The dissipation  $DI \leq 0$  and given by

$$DI = -2v(u^T(M_x H_y + H_x M_y)u + v^T(M_x H_y + H_x M_y)v).$$

The term  $RT = u^T(A_x + B_y)\bar{H}u + v^T(A_x + B_y)\bar{H}v + (D_x u + D_y v)^T \bar{H}p$  is proportional to the discrete divergence. To obtain (41) we used the two assumptions: (i)  $H$  is a diagonal norm, and (ii)  $M_x, M_y$  are symmetric positive semi-definite. Note also that  $(A_x + B_y)$  is equivalent to  $(D_x u + D_y v)$  in the nonlinear case.

The boundary terms ( $BT \equiv BT_w + BT_e + BT_s + BT_n$ ) are given by

$$\begin{aligned} BT_w &= +u_w^T H(u_w - 2\tau_w^{(u)} \lambda_5^{(w)})u_w + 2u_w^T H(1 + \tau_w^{(u)})(p_w - v(Su)_w) + v_w^T H(v_w - 2\tau_w^{(v)} \lambda_2^{(w)})v_w \\ &\quad + 2v_w^T H(1 + \tau_w^{(v)})(-v(Sv)_w), \\ BT_e &= -u_e^T H(u_e - 2\tau_e^{(v)} \lambda_5^{(e)})u_e - 2u_e^T H(1 - \tau_e^{(u)})(p_w - v(Su)_e) - v_e^T H(v_w - 2\tau_e^{(v)} \lambda_2^{(e)})v_e \\ &\quad - 2v_e^T H(1 - \tau_e^{(v)})(-v(Sv)_e), \\ BT_s &= +v_s^T H(v_s - 2\tau_s^{(v)} \lambda_5^{(s)})v_s + 2v_s^T H(1 + \tau_s^{(v)})(p_s - v(Sv)_s) + u_s^T H(u_s - 2\tau_s^{(u)} \lambda_2^{(s)})u_s \\ &\quad + 2u_s^T H(1 + \tau_s^{(u)})(-v(Su)_s), \\ BT_n &= -v_n^T H(v_n - 2\tau_n^{(u)} \lambda_5^{(n)})v_n - 2v_n^T H(1 - \tau_n^{(v)})(p_n - v(Sv)_n) - u_n^T H(u_n - 2\tau_n^{(u)} \lambda_2^{(n)})u_n \\ &\quad - 2u_n^T H(1 - \tau_n^{(u)})(-v(Su)_n). \end{aligned}$$

$BT$  can clearly be bounded if and only if  $\tau_{w,s}^{(u,v)} = -1$  and  $\tau_{e,n}^{(u,v)} = 1$ . That leads to:

$$BT = \begin{cases} -u_w^T(H\sqrt{u_w^2 + 8})u_w - v_w^T(H\sqrt{v_w^2 + 4})v_w, \\ -u_e^T(H\sqrt{u_e^2 + 8})u_e - v_e^T(H\sqrt{v_e^2 + 4})v_e, \\ -v_s^T(H\sqrt{v_s^2 + 8})v_s - u_s^T(H\sqrt{u_s^2 + 4})u_s, \\ -v_n^T(H\sqrt{v_n^2 + 8})v_n - u_n^T(H\sqrt{u_n^2 + 4})u_n \end{cases} \tag{42}$$

and an energy estimate completely analogous to the continuous case. (To realize that  $\|C^+\|_r^2 = \sum_{i=1,3,4} \oint_r \lambda_i C_i^2 ds$  in (18) corresponds to (42), solve for the gradients in (17) and insert them in  $\|C^+\|_r^2$ .)

### 4.3. Solving the Poisson system for the pressure

Closing the system (36) requires appropriate boundary condition for the pressure. We will very briefly outline the procedure to compute a modified pressure that is consistent with the maximally dissipative divergence boundary condition (37) and the momentum boundary conditions (38) and (39). The procedure for the west (or the east) boundary is as follows:

- (1) Use (39) to extract the tangential component of velocity ( $\tilde{v}_w$ ) at the boundary.
- (2) Use (37) and  $\tilde{v}_w$  to compute the normal component of velocity ( $\tilde{u}_w$ ) at the boundary.
- (3) Use (38),  $\tilde{v}_w$  and  $\tilde{u}_w$  to compute the pressure ( $\tilde{p}_w$ ) at the boundary.

Similarly, the procedure for the south (or the north) boundary is given by

- (1) Use (38) to extract the tangential component of velocity ( $\tilde{u}_s$ ) at the boundary.
- (2) Use (37) and  $\tilde{u}_s$  to compute the normal component of velocity ( $\tilde{v}_s$ ) at the boundary.
- (3) Use (39),  $\tilde{u}_s$  and  $\tilde{v}_s$  to compute the pressure ( $\tilde{p}_s$ ) at the boundary.

Once the pressure at the boundaries is determined, we can close the Poisson system. First we multiply (36) with  $\overline{H} \equiv H_x H_y$ , to obtain

$$((-M + BS \otimes H) + (H \otimes -M + BS))p = \overline{H}f.$$

Next we use  $\tilde{p}_{w,e,s,n}$  (obtained in the procedure described above) to reduce it to a system where only the interior points are included (denoted by the tilde sign). The resulting nonsingular positive definite symmetric reduced system can be written

$$(\tilde{M} \otimes \tilde{H} + \tilde{H} \otimes \tilde{M})\tilde{p} = -\tilde{H}f - BT, \tag{43}$$

where  $BT = (\tilde{M}_w \otimes \tilde{H})\tilde{p}_w + (\tilde{M}_e \otimes \tilde{H})\tilde{p}_e + (\tilde{H} \otimes \tilde{M}_s)\tilde{p}_s + (\tilde{H} \otimes \tilde{M}_n)\tilde{p}_n$ . The matrices  $\tilde{M}_{w,s}$  and  $\tilde{M}_{e,n}$  denote the first and last column of  $M$ , excluding the first and last row. The nonzero elements in the boundary derivative operator  $BS$  (see Definition 4.2) sits in the first and the last row. The dissipative part  $M$  is by construction symmetric and positive semi-definite. By removing the first and last rows and the first and last columns in  $-M + BS$ , it is reduced to  $-\tilde{M}$ . It can be shown that  $\tilde{M}$  is positive definite.

**Remark.**

Due to the symmetric positive definiteness of (43), it can be solved efficiently. For our small scale problem, we used the *LU* decomposition technique. Other choices for small scale problems are the incomplete Cholesky or the preconditioned conjugate gradient method. For large scale problems running in parallel, multi grid (for example provided in the software package *hypr* [27]) would be more appropriate.

**Remark.** The system (43) requires known pressure values at the boundaries. At solid boundaries, the normal derivative of the pressure can be used to compute the pressure at the boundary, see [5] for details.

## 5. Computations

We will test our method on the analytic Taylor vortex model given by

$$\begin{aligned} u &= -\cos(\alpha) \sin(\beta) \exp(-2\pi^2 vt) + u_\infty \cos(\theta), \\ v &= \sin(\alpha) \cos(\beta) \exp(-2\pi^2 vt) + u_\infty \sin(\theta), \\ p &= -\frac{1}{4}(\cos(2\alpha) + \cos(2\beta)) \exp(-4\pi^2 vt), \\ \alpha &= \pi(x - x_0 - u_\infty \cos(\theta)t), \quad \beta = \pi(y - y_0 - u_\infty \sin(\theta)t). \end{aligned} \tag{44}$$

The Taylor vortex is an analytic solution to the incompressible Navier–Stokes equations. In (44),  $(x_0, y_0)$  is the initial position,  $u_\infty$  is the free-stream value and  $\theta$  the direction of the flow. The vortex is introduced into the computational domain by using the analytic solution as boundary data and initial data.

For time advancement we use the explicit standard fourth-order Runge–Kutta method. The (inviscid) time-step choice  $\Delta t = \Delta x/2$  was stable in all calculations for  $\nu = 0.01$ . For much larger  $\nu$  and/or for much higher resolutions, the viscid stability restrictions starts to apply, and an explicit Chebyshev Runge–Kutta method [26] might be more effective.

In all the calculations below we use  $\nu = 0.01$  and a fifth-order scheme (sixth-order interior accuracy and third-order at boundaries). The pressure and streamline contours calculated on the  $41^2$  mesh at  $T = 0.4$  are shown in Fig. 2.

The convergence results at  $T = 1$  for  $u, v, p$  and the divergence are shown in Tables 1 and 2. The divergence is calculated using  $D_x u + D_y v$  with the fifth-order scheme. Both calculations use (38) and (39) as boundary conditions. BC0 uses a Dirichlet condition on the divergence as the third condition. BC1 uses the advection–diffusion condition (37) as the third condition. Both conditions are acceptable in the sense that they do not contribute to growth of the divergence for the continuous problem.

The correct order of accuracy is obtained for all variables. Also, as could be expected, the order of accuracy of the divergence seem to be approximately one order less compared to the one obtained for the variables. The results are similar with a slight advantage for BC1.

The time evolution (decay as predicted by the theory in this paper) of the divergence and  $l_2$ -error of the kinetic energy are shown in Fig. 3, see also Table 3. Both calculations were initiated using the exact analytical solution (44) injected in the grid points. The result is very similar for the two types of boundary conditions and in both cases, the divergence is clearly decreasing. BC1 performs marginally better.

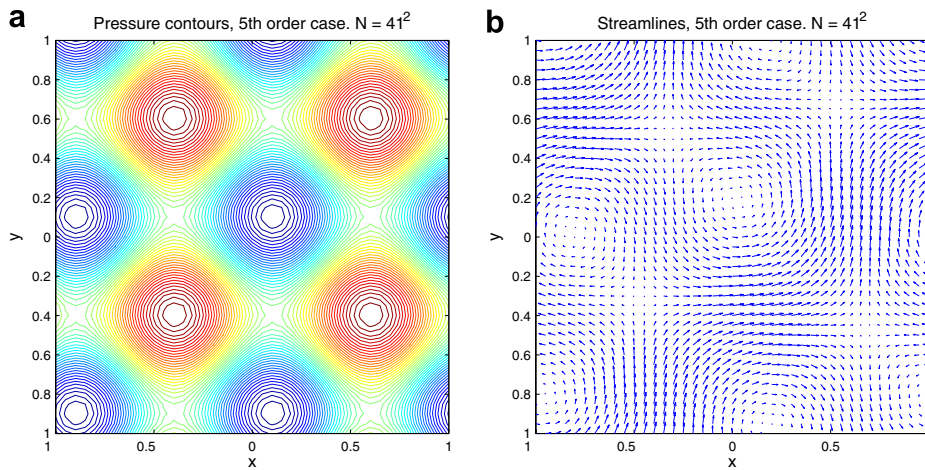


Fig. 2. Pressure contour and streamlines at  $T = 0.4$ ,  $N = 41^2$ ,  $\nu = 0.01$ . (a) Pressure and (b) streamlines.

Table 1  
 $l_2$ -error and convergence rate  $q$ ,  $T = 1$

$N$	$\log(l_2(u))$	$q^{(u)}$	$\log(l_2(v))$	$q^{(v)}$	$\log(l_2(p))$	$q^{(p)}$	$\log(l_2(\text{div}))$	$q^{(\text{div})}$
21	-2.50	0.00	-2.49	0.00	-2.46	0.00	-1.30	0.00
41	-3.85	4.51	-3.92	4.76	-3.90	4.79	-2.55	4.17
61	-4.67	4.65	-4.75	4.73	-4.76	4.88	-3.27	4.07
81	-5.29	4.92	-5.37	4.93	-5.37	4.87	-3.75	3.87
101	-5.77	5.02	-5.85	5.02	-5.84	4.85	-4.11	3.71
151	-6.67	5.15	-6.74	5.10	-6.68	4.81	-4.74	3.61

Dirichlet boundary condition,  $\nu = 0.01$ .

Table 2  
 $l_2$ -error and convergence rate  $q$ ,  $T = 1$

$N$	$\log(l_2(u))$	$q^{(u)}$	$\log(l_2(v))$	$q^{(v)}$	$\log(l_2(p))$	$q^{(p)}$	$\log(l_2(\text{div}))$	$q^{(\text{div})}$
21	-2.09	0.00	-2.09	0.00	-2.23	0.00	-0.62	0.00
41	-3.87	5.90	-3.86	5.89	-4.03	6.01	-2.15	5.09
61	-4.84	5.51	-4.83	5.51	-5.04	5.72	-3.03	4.98
81	-5.50	5.33	-5.50	5.35	-5.70	5.31	-3.61	4.59
101	-6.02	5.29	-6.01	5.31	-6.20	5.13	-4.02	4.26
151	-6.95	5.32	-6.95	5.38	-7.10	5.15	-4.71	3.95

Advection–diffusion BC,  $\nu = 0.01$ .

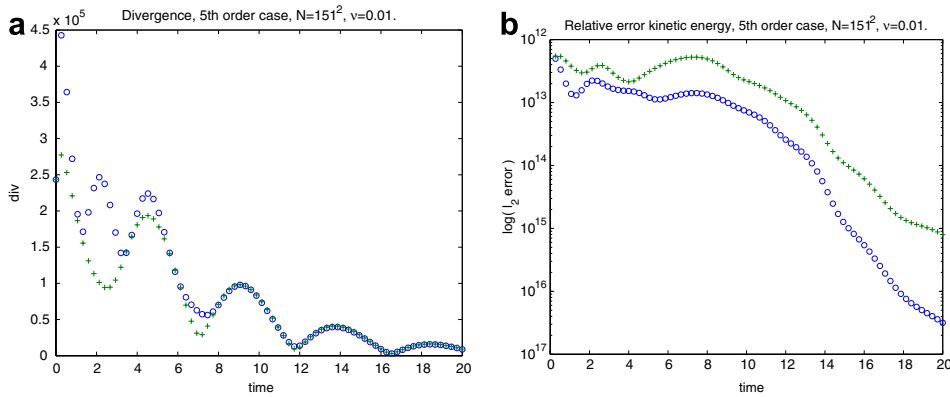


Fig. 3. Time history for divergence and  $l_2$  error of kinetic energy,  $N = 151^2$ . The initial solution is the exact continuous solution. Circles are BC1,  $\nu = 0.01$ . (a) Divergence and (b) kinetic energy.

Table 3  
 $l_2$ -error at  $T = 20$ ,  $N = 151^2$ ,  $\nu = 0.01$

BC	$\log(l_2(u))$	$\log(l_2(v))$	$\log(l_2(p))$	$\log(l_2(\text{div}))$	$\log(l_2(u^2 + v^2))$
BC0	-8.41	-8.23	-8.67	-6.42	-16.14
BC1	-9.23	-8.94	-9.51	-6.43	-17.54

Two different boundary conditions.

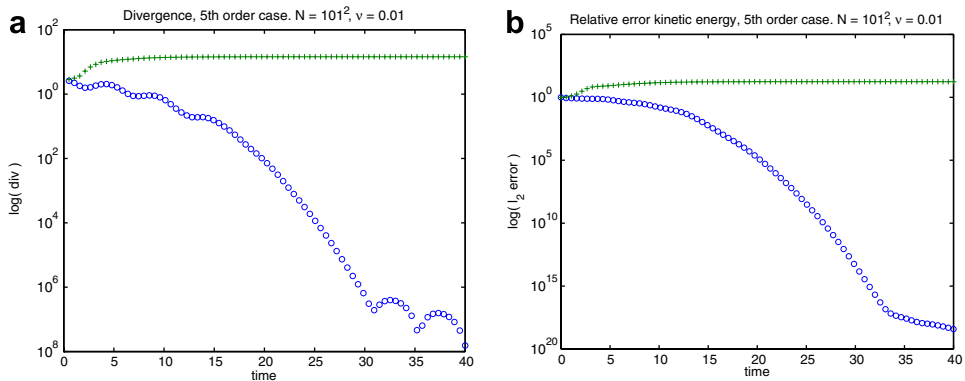


Fig. 4. Time history for divergence and  $l_2$  error of kinetic energy,  $N = 101^2$ . The initial solution is far from the exact continuous solution. Circles are BC1,  $\nu = 0.01$ , (a) Divergence and (b) kinetic energy.

Table 4

$l_2$ -error at  $T = 40$ ,  $N = 101^2$ ,  $\nu = 0.01$

<i>BC</i>	$\log(l_2(u))$	$\log(l_2(v))$	$\log(l_2(p))$	$\log(l_2(\text{div}))$	$\log(l_2(u^2 + v^2))$
<i>BC0</i>	-0.09	-0.09	0.02	0.79	0.20
<i>BC1</i>	-9.97	-9.97	-10.81	-8.19	-19.47

Two different boundary conditions.

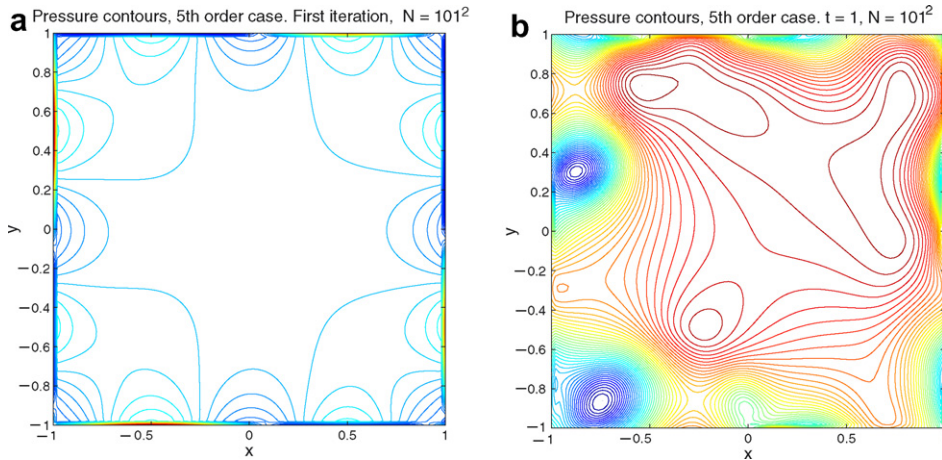


Fig. 5. Snapshots of pressure distribution using BC1,  $N = 101^2$ ,  $\nu = 0.01$ . (a) Pressure,  $T = \Delta t$  and (b) pressure,  $T = 1$ .

As a final test we initialized the two calculations above with the initial data  $u = v = 0$  and  $p = 1$ . We used exact boundary data given by (44). This means that the initial data is far from the exact solution. The homogeneous initial conditions are incompatible with the boundary data from the exact solution, which generates a nonsmooth solution with very large numerical divergence right next to the boundary.

The time evolution of the divergence and  $l_2$ -error of the kinetic energy are shown in Fig. 4, see also Tables 4. This time the result using BC1 is clearly superior with a fast convergence towards the analytical solution. BC0 does not converge to the analytical solution. The convergence of the calculation using BC1 is further illustrated in Figs. 5–7. This final test illustrates the remark just before Section 2.2 which states that initial nonzero

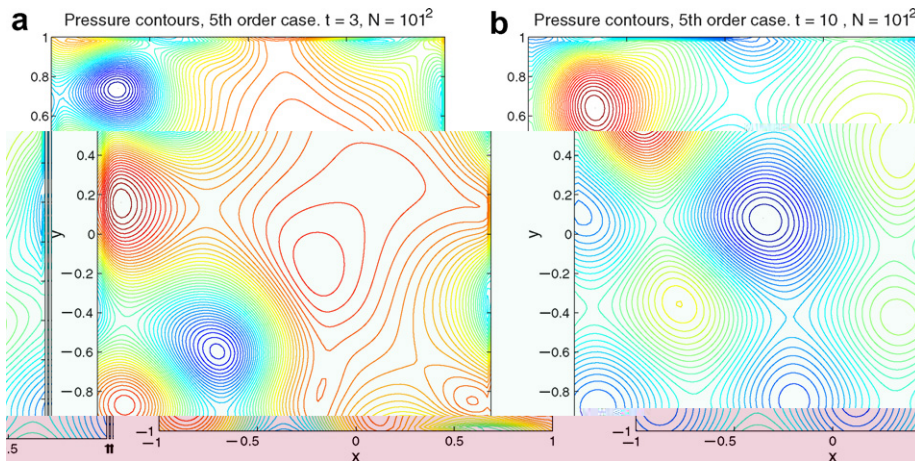


Fig. 6. Snapshots of pressure distribution using BC1,  $N = 101^2$ ,  $\nu = 0.01$ . (a) Pressure,  $T = 3$  and (b) pressure,  $T = 10$ .

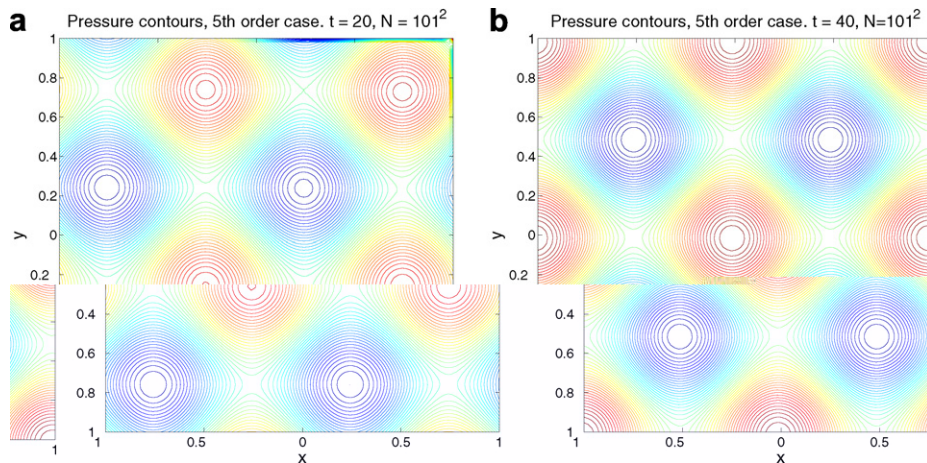


Fig. 7. Snapshots of pressure distribution using BC1,  $N = 101^2$ ,  $\nu = 0.01$ . (a) Pressure,  $T = 20$  and (b) pressure,  $T = 40$ .

divergence effects might decay with time, by using a sufficiently dissipative boundary condition. Note that there are both decay and growth terms in (4).

**Remark.** In the test problem above we have different boundary conditions with exact boundary data. Since the boundary conditions are different we cannot prove that we have only one solution. However, it is likely since both versions of the boundary conditions lead to well-posedness for the separate linearized problems.

## 6. Conclusions

The nonlinear velocity–pressure formulation of the incompressible Navier–Stokes equations is analyzed. New sets of boundary conditions are derived. The boundary conditions have the same form on both inflow and outflow boundaries and lead to a divergence free solution.

The new boundary conditions are applied to a constant coefficient problem, where the solution in Laplace–Fourier space can be written down explicitly. It is shown that the velocity–pressure formulation with the new boundary conditions yield a divergence free solution and that all dependent variables including the pressure is bounded.

The new formulation were implemented numerically using summation-by-parts operators and penalty technique. Stability of the linearized problem was shown. It was also shown how to use the new boundary conditions to obtain consistent pressure values on the boundary, necessary for obtaining a symmetric positive definite Poisson system.

The numerical procedure was tested on an analytical solution to the Navier–Stokes equations and stability as well as the correct order of accuracy were demonstrated. As predicted by the theory, the initial divergence in the solution decays, and as time passes a more and more divergence free and accurate solution is obtained. This process is much more pronounced for the most dissipative variant of the boundary conditions.

## References

- [1] P.M. Gresho, R.L. Sani, On pressure boundary conditions for the incompressible Navier–Stokes equations, *Int. J. Numer. Methods Fluids* 7 (1987) 1111–1145.
- [2] W.D. Henshaw, A fourth-order accurate method for the incompressible Navier–Stokes equations on overlapping grids, *J. Comput. Phys.* 113 (1994) 13–25.
- [3] W.D. Henshaw, H.-O. Kreiss, L.G.M. Reyna, A fourth-order accurate difference approximation for the incompressible Navier–Stokes equations, *Comput. Fluids* 23 (4) (1994) 575–593.
- [4] J. Strikwerda, Finite difference methods for the Stokes and Navier–Stokes equations, *SIAM J. Sci. Stat. Comput.* 5 (1984) 56–68.
- [5] N.A. Petersson, Stability of pressure boundary conditions for Stokes and Navier–Stokes equations, *J. Comput. Phys.* 172 (2001) 40–70.

- [6] A. Bruger, B. Gustafsson, P. Lstedt, J. Nilsson, High order accurate solution of the incompressible Navier–Stokes equations, *J. Comput. Phys.* 203 (2005) 49–71.
- [7] B. Gustafsson, J. Nilsson, Boundary conditions and estimates for the Stokes equations on staggered grids, *J. Sci. Comput.* 15 (2000) 29–54.
- [8] B. Gustafsson, J. Nilsson, Fourth order methods for the Stokes and Navier–Stokes equations on staggered grids, in: D.A. Cagney, M.M. Hafez (Eds.), *Frontiers of Computational Fluid Dynamics-2002*, World Scientific, Singapore, 2002, pp. 165–179.
- [9] W. Kress, J. Nilsson, Boundary conditions and estimates for the linearized Navier–Stokes equations on a staggered grid, *Comput. Fluids* 32 (2003) 1093–1112.
- [10] W. Chang, F. Giraldo, B. Perot, Analysis of an exact fractional step method, *J. Comput. Phys.* 180 (2002) 183–199.
- [11] J.C. Strikwerda, Y.S. Lee, The accuracy of the fractional step method, *SIAM J. Numer. Anal.* 37 (1) (1999) 37–47.
- [12] J. Kim, P. Moin, Application of a fractional-step method to incompressible Navier–Stokes equations, *J. Comput. Phys.* 59 (1985) 308–323.
- [13] C. Johansson, Boundary conditions for open boundaries for the incompressible Navier–Stokes equations, *J. Comput. Phys.* 105 (1993) 233–251.
- [14] J. Nordström, M. Svård, Well posed boundary conditions for the Navier–Stokes equation, *SIAM J. Numer. Anal.* 43 (3) (2005) 1231–1255.
- [15] H.O. Kreiss, J. Lorenz, *Initial Boundary Value Problems and the Navier–Stokes Equations*, Academic Press, New York, 1989.
- [16] J. Nordström, N. Nordin, D.S. Henningson, The fringe region technique and the Fourier-method used in the direct numerical simulation of spatially evolving viscous flows, *SIAM J. Sci. Comput.* 20 (4) (1999) 1365–1393.
- [17] J.W. Slater, Verification assessment of flow boundary conditions for CFD analysis of supersonic inlet flows, *AIAA Paper* 2001-3882, 2001.
- [18] A. Jirasek, Mass flow boundary conditions for subsonic inflow and outflow boundaries, *AIAA J.* 44 (5) (2006).
- [19] U. Trottenberg, C.W. Oosterlee, A. Schüller, *Multigrid*, Academic Press, 2001.
- [20] H.-O. Kreiss, G. Scherer, Finite element and finite difference methods for hyperbolic partial differential equations, in: C. De Boor (Ed.), *Mathematical Aspects of Finite Elements in Partial Differential Equation*, Academic Press, New York, 1974.
- [21] B. Strand, Summation by parts for finite difference approximation for  $d/dx$ , *J. Comput. Phys.* 110 (1994) 47–67.
- [22] K. Mattson, J. Nordström, Summation by parts operators for finite difference approximations of second derivatives, *J. Comput. Phys.* 199 (2004) 503–540.
- [23] M. Svård, J. Nordström, On the order of accuracy for difference approximations of initial-boundary value problems, *J. Comput. Phys.* 218 (2006) 333–352.
- [24] M.H. Carpenter, D. Gottlieb, S. Abarbanel, Time-stable boundary conditions for finite-difference schemes solving hyperbolic systems: methodology and application to high-order compact schemes, *J. Comput. Phys.* 129 (1994).
- [25] M.H. Carpenter, J. Nordström, D. Gottlieb, A stable and conservative interface treatment of arbitrary spatial accuracy, *J. Comput. Phys.* 148 (1999) 341–365.
- [26] A.A. Medovikov, High order explicit methods for parabolic problems, *BIT* 38 (2) (1998) 372–390.
- [27] R.D. Falgout, J.E. Jones, U.M. Yang, The design and implementation of hypre, a library of parallel high performance preconditioners, in: A.M. Bruaset, A. Tveito (Eds.), *Numerical Solution of Partial Differential Equations on Parallel Computers*, vol. 51, Springer-Verlag, 2006, pp. 267–294.